J Therm Anal Calorim (2009) 98:785–792
DOI 10.1007/s10973-009-0205-2

Synthesis, characterization and thermal study of some tetradentate Schiff base transition metal complexes

Fatih Doğan · Mahmut Ulusoy · Ömer F. Öztürk · İsmet Kaya · Bekir Salih

Received: 19 March 2009 / Accepted: 5 June 2009 / Published online: 28 August 2009

Abstract Several mononuclear Co(II), Ni(II), Cu(II), and Fe(II) complexes of tetradentate salpren-type diimine, obtained from 3,5-di-*tert*-butyl-2-hydroxybenzaldehyde and 1,3-diaminopropane have been prepared and characterized by analytical, spectroscopic (FT-IR, UV–VIS) techniques, magnetic susceptibility measurements and thermogravimetric analyses (TG). The thermodynamic and thermal properties of complexes have been investigated. For further characterization Direct Insertion Probe-Mass Spectrometry (DIP-MS) was used and the fragmentation pattern and also stability of the ions were evaluated. The characterization of the end products of the decomposition was achieved by X-ray diffraction. The thermal stabilities of metal complexes of *N*,*N*′-bis(3,5-di-*t*-butylsalicylidene)-1,3-propanediamine ligand (**L**) were found as Ni(II) > Cu(II) > Co(II) > Fe(II).

Keywords Activation energy · Sterically hindered diimine · Thermal decomposition · Transition metal complexes

F. Doğan (✉)
Faculty of Education, Secondary Science and Mathematics Education, Çanakkale Onsekiz Mart University, 17020 Canakkale, Turkey
e-mail: fatihdogan@comu.edu.tr

M. Ulusoy
Department of Chemistry, Faculty of Science, Ege University, 35100 Izmir, Turkey

Ö. F. Öztürk · İ. Kaya
Department of Chemistry, Çanakkale Onsekiz Mart University, 17020 Canakkale, Turkey

B. Salih
Department of Chemistry, Faculty of Science, Hacettepe University, Ankara, Turkey

Introduction

Intermolecular electron transfer is a fundamental chemical phenomenon and relates specifically to redox processes which occur in both natural and synthetic electron-transfer systems [1]. The ability of metal ions to control the oxidation potentials of organic molecules by complexation has a significant role in biological electron-transfer processes, molecular electronics and also in catalysis [2]. The Ni(II) ions play a central role in biological redox metalloenzymes like plastocyanin, hemocyanin, azurin, galactose oxidase and others [3]. It should be noted that while the chemistry of metal complexes with salen-type and other polydentate ligands bearing 2,4-*t*-butyl moieties has been extensively studied because of their efficient catalytic activity and their use as model complexes for metalloproteinase having metal centers and proximal organic radicals in their active site[4]. Tetradentate Schiff base complexes have been extensively studied. Kumar [5] has investigated the thermal stabilities of some new cobalt complexes. The decomposition mechanism and kinetic parameters of a complex of *N*,*N*′-etylenebis(salicylideneiminato) diaquochromium(III) nitrate, $[Cr(salen)(H_2O)]NO_3$ was studied by Wang [6]. Also, Doğan et.al. [7, 8] have investigated the thermal behavior, kinetic and thermodynamic parameters of various metal complexes and salts using TG/DTG, DTA.

In the present work, the synthesis, spectroscopic characterization of the Cu(II), Ni(II), Co(II) and Fe(II) complexes from Schiff base (**L**) formed from 3,5-di-*tert*–butyl-2-hydroxybenzaldehyde and 1,3-diaminopropane are reported except Cu(II) and Ni(II) complexes since they have been published before [9] and we have also investigated thermal behaviors and thermodynamic properties of synthesized complexes to understand the mechanisms of decomposition and thermodynamic parameters. In the decomposition

kinetic study, the integral methods employing the Coats–Redfern [10], van Krevelen [11], MacCallum–Tanner [12], Madhusudanan–Krishnan–Ninan equations [13] and the approximation method Horowitz–Metzger equation [14] were used for the calculation of kinetic and thermodynamic parameters such as the reaction order n, the activation energy E, the pre-exponential factor A, the entropy change $\Delta S^{\#}$, the enthalpy change $\Delta H^{\#}$, and the Gibbs free change $\Delta G^{\#}$. Also the heat capacity is calculated from the results of differential scanning calorimetry (DSC).

Experimental

Instrumental

3,5-di-*tert*–butyl-2-hydroxybenzaldehyde (3,5-DTB) was synthesized according to the literature procedure [15], 1,3-diaminopropane is purchased from Aldrich (pure) and used without purification. The elemental analyses were determined in the TUBİTAK Laboratory (Turkish Scientific and Technological Research Council), IR spectra were recorded on a Perkin Elmer Spectrum RXI FT-IR Spectrometer as KBr pellets, Magnetic Susceptibilities were determined on a Sherwood Scientific Magnetic Susceptibility Balance (Model MK1) at room temperature (20 °C) using $Hg[Co(SCN)_4]$ as a calibrant; diamagnetic corrections were calculated from Pascal's constants [16], UV spectra were recorded on a Schimadzu 1601 PC. The residual end products of heating were identified by X-ray powder diffractometry using a Rigaku DMAX 2200 XRD instrument (Cu lamp, $\lambda_{K\alpha} = 1{,}5418$, Rigaku, Tokyo, Japan). Thermogravimetric (DTG/TG) curves were performed on a Seteram Labsys TG-16 thermobalance, operating in dynamic mode, with the following conditions; sample mass $\sim$5 mg, heating rate = 10 °C/min, atmosphere of nitrogen (10 cm^3 min^{-1}), sealed platinum pan. The DSC curves were obtained using DSC–60 Schimadzu apparatus (heating rates of 10 °C/min, aluminum crucible, mass $\sim$5 mg, in nitrogen atmosphere).

Ligand (**L**) and its metal ion complexes, such as Co(II), Ni(II), Cu(II) and Fe(III)-complexes, were analyzed using Agilent 5973 Inert Mass Selective Detector equipped with Direct Insertion Probe (HPP7&ProbeDirect, Scientific Instrument Services, Ringoes, NJ USA). About 1 mg of the ligand and its complexes were weighted and then inserted inside the quartz sample tube (Scientific Instrument Services, Ringoes, NJ USA) that was used for inserting the sample inside mass spectrometer. At the mass spectrometer part, Electron Impact Ionization (EI) source was used, the temperature of the source was set to 140 °C, vacuum was 1.5×10^{-6} Torr during the recording of mass spectra. The Direct Insertion Probe program was set as given below:

Initial temperature was set to 50 °C for 10 min and then temperature was increased up to 420 °C with 10 °C min^{-1} temperature ramp. Finally temperature was hold at 420 °C for 50 min.

Synthesis of Co(II) and Fe(II) complexes

One mmole *N*,*N*′-bis(3,5-di-*t*-butylsalicylidene)-1,3-propanediamine was dissolved in 30 mL absolute methanol and 1 mmole $Co(OAc)_2 \cdot 4H_2O$ or $FeCl_2 \cdot 4H_2O$ in 10 mL methanol were mixed. Desired products were precipitated immediately. The stirred mixture was refluxed for 60 min. The mixture was evaporated to 15–20 mL left to cool to room temperature. The complexes were filtered off, washed with a small amount of methanol/H_2O (1:1) and filtered in vacuo again. All complexes recrystallized in CH_2Cl_2/Ethanol(1/3).

Results and discussions

Characterization of Co(II) and Fe(II) complexes

The analytical data for all these were presented in Table 1. In the spectrum of ligand, a strong band observed in the IR spectra of the free ligand in 1,630 cm^{-1} region which is attributed to the C=N strech, showed a negative shift to ca. 1,615–1,623 cm^{-1} in the spectra of all the complexes, indicating coordination of the azomethine nitrogen atom to metals [17]. The salpren ligand shows a strong and broad OH band centered at 3,400 cm^{-1} due to the phenolic O–H bonds. The position and the broadness of the band are indicative of hydrogen bonding between the phenolic protons and the imine nitrogen atoms. This OH band disappeared while the complexation of the ligand with Co(II) ion due to breaking off the phenolic protons. On the other hand, Fe(II) (salpren) complex shows a broad band at 3,446–3,346 cm^{-1} indicating the coordination of water molecule to metal center. The decomposition temperature and the mass losses of the complexes were calculated from the TGA data. Observed mass loss for the Fe(II) (salpren) complex from the TGA data is 3.14%. This suggests that Fe(II) (salpren) complex has 1 mole water per complex molecule in the coordination sphere. This is also supported by the elemental analysis data. The structure recommended is shown in Scheme 1.

The electronic spectral data of the synthesized ligand was recorded in chloroform solutions. In the spectrum of the Schiff base ligand, the aromatic bands at 220–265 nm are attributed to a benzene $\pi \rightarrow \pi^*$ transition. The band at 425 nm is assigned to the imino $\pi \rightarrow \pi^*$ or $n \rightarrow \pi^*$ transition [18]. The electronic Spectra of the complexes were examined in chloroform solvent. The bands below 420 nm have very high extinction coefficients and are almost certainly associated with intraligand $\pi \rightarrow \pi^*$ and $n \rightarrow \pi^*$

Table 1 The colors, formulas, formula masses, melting points, magnetic susceptibilities, yields and elemental analyses results of the complexes

Compounds	F.W./g mol^{-1}	Color	m.p./°C	Yield/%	μ_{eff} [B.M]	Elementel analyses/% calculated (found) C	H	N
Co(II) (salpren) $C_{33}H_{48}N_2O_2Co$	563.68	Dark brown	153	73	1.8	70.32 (70.65)	8.58 (8.64)	4.97 (4.50)
Fe(II) (salpren) $C_{33}H_{50}N_2O_3Fe$	78.61	Purple	158	68	5.35	68.50 (68.33)	8.71 (8.56)	4.84 (4.54)

Scheme 1 Synthetic route to the metal complexes

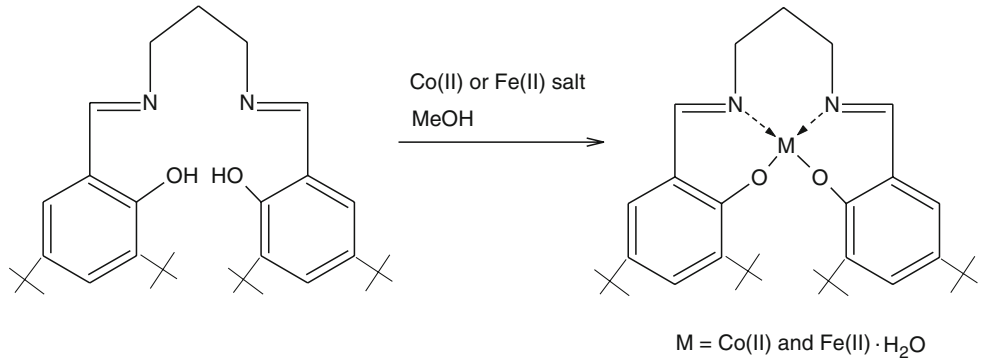

Table 2 IR and electronic spectral data for salpren, Co(II) and Fe(II) (salpren) complexes

Compounds	IR spectra/cm^{-1}		Electronic spectra*/λ nm^{-1}				
	υO–H	υC = N					
Salpren	3,410	1,630	230	263	332	425*	
Co(II) (salpren)	–	1,623	266	356	406	512*	644*
Fe(II) (salpren)	3,446 (H_2O)	1,615	274	330	533	605*	

*Shoulder

transitions, and absorptions at 420–500 nm are assigned to metal-to-ligand charge transfer (MLCT) transitions. The weak shoulder bands over 500 nm is because of the d → d transitions. The colors, formulas, formula masses, melting points, magnetic susceptibilities, yields, elemental analyses, IR and electronic spectral data obtained for the compounds described in this work are summarized in Tables 1 and 2. The magnetic behavior of the Fe(II) complex of salpren is consistent with the fact that this complex has four unpaired electrons and suggests that they have distorted structures with considerable delocalization.

Magnetic moments (4.09 BM) of the cobalt(II) complex at room temperature, which suggests a spin quartet state $S = 3/2$ in a tetrahedral geometry [19]. According to the electronic spectrum and magnetic measurements the iron atom is pentacoordinated in a square-pyramidal geometry, with the tetradentate salpren ligand in a square planar coordination, by two nitrogen and two oxygen atoms, with the aqua ligand in an apical position [20].

GC-MS studies

Mass spectrum of **L** is given in Fig. 1 with the total ion chromatogram of **L**. On the total ion chromatogram, beside the main peak of the ligand obtained at 5.6 min retention time, some other decomposition peaks were observed. When the mass spectrum of the main peak on the total ion chromatogram was evaluated, it was noticed that this compound corresponded to the mass spectrum of **L** exactly. In the mass spectrum given in Fig. 1b, the peaks appeared at 506, 491, 260, 246, 219, 232, 57 and 238 atomic masses characterized the M^+, $[M\text{-}15]^+$, $[C_{17}H_{26}NO]^+$, $[C_{16}H_{24}NO]^+$, $[C_{16}H_{24}NO\text{-}27]^+$, $[C_{17}H_{26}NO\text{-}28]^+$, $[(CH_3)_3C]^+$ and $[M\text{-}15\text{-}15]^{2+}$. Especially, the peak with high intensity at 238 nominal atomic mass is really interesting and represents a very stable doubly charged ion of the ligand in EI-Mass spectrometry, which is unexpected. The doubly charged ion's stability is because of the high volume of ligand and the charged locations are far enough away from each other to eliminate charge repulsion.

When mass spectra of metal complexes of this ligand were interpreted, similar fragmentations were observed but doubly charged ion intensity of the complexes accompanied by the elimination or two methyl groups from both bulky sides of the complexes were found to be higher than the intensity of the same peak of pure ligand. For the metal complexes, the mass of the peaks observed on mass spectra with their per cent intensities are given in Table 3.

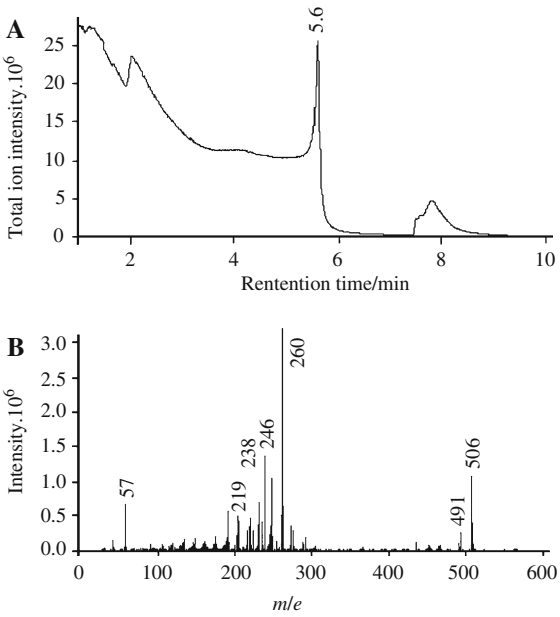

Fig. 1 Total ion chromatogram (**a**) and mass spectrum of L ligand (**b**). Mass spectrum was obtained at 5.6 retention time

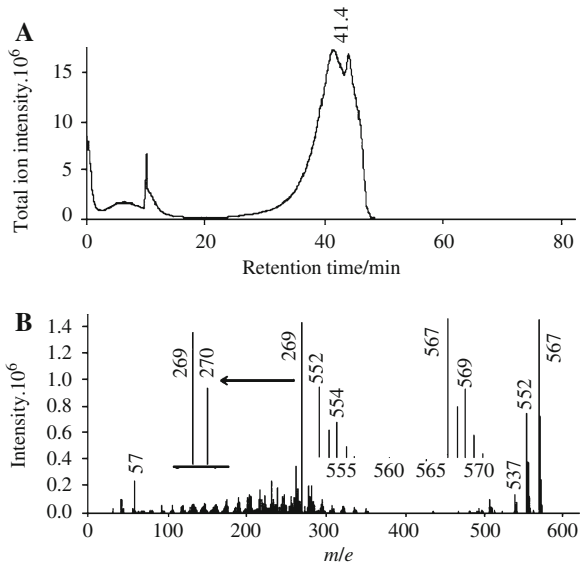

Fig. 2 Total ion chromatogram (**a**) and mass spectrum of L-Cu (II) complex (**b**). Mass spectrum was obtained at 41.4 retention time

In order to evaluate the high intense doubly charged ion which is overlapped with one intense fragment ion of the pure ligand further, mass spectra of copper complex of **L** with the total ion mass chromatogram of the complex is given in Fig. 2. Following the isotopic peak masses and intensities of copper in the complex, the stability of doubly charged ion intensity yielded from metal complex of **L** could be examined. Evaluating the isotopic peak masses and intensities of copper in either single charge molecular ion or doubly charged molecular ion form, the presence of doubly charged ions in the spectrum could be examined clearly. Single charged molecular ions at 567 and 569 nominal masses are the M^+ and $[M + 2]^+$ characterizing the most abundant copper isotopes, which have ^{63}Cu and ^{65}Cu with 69.17% and 30.83% naturally abundance. The doubly charged ion of the complex formed upon the leaving of two methyl groups from both bulky sides of the complex yielded again two peaks appeared at 269 and 270 nominal masses again showing the copper isotope distribution with ^{13}C. These results clearly show that complex yields high intense (very stable) double charged ion loosing two methyl groups.

Thermodynamic and thermal studies

The complexes exhibited an endothermic process. The area of the endothermic peak corresponds to the heat of fusion and the peak temperature corresponds to the melting point. The melting (T_p) and transition temperatures (T_1, T_2) of the complexes are given in Table 4. The heat capacities C_p of

Table 3 Mass and intensity (%) of the peaks were evaluated from mass spectra of the studied complexes

Cobalt complex			Nickel complex			Iron complex			Copper complex		
Nominal mass	Intensity	Type of ion	Nominal mass	Intensity	Type of ion	Nominal mass	Intensity	Type of ion	Nominal mass	Intensity	Type of ion
563	100	M^+	562	100	M^+	560	100	$[M + 2]^+$	567	97.8	M^+
267	77.9	$[M\text{-}15\text{-}15]^{2+}$	266	79.8	$[M\text{-}15\text{-}15]^{2+}$	265	50.4	$[M\text{-}15\text{-}15 + 2]^{2+}$	269	100	$[M\text{-}15\text{-}15]^{2+}$
548	62.5	$[M\text{-}15]^+$	547	56.3	$[M\text{-}15]^+$	545	34.5	$[M\text{-}15]^+$	270	56.9	$[M\text{-}15\text{-}15 + 2]^{2+}$
57	24.7	$[(CH_3)_3C]^+$	564	46.0	$[M + 2]^+$	57	16.7	$[(CH_3)_3C]^+$	552	50.9	$[M\text{-}15 + 2]^+$
260	12.2	$[C_{17}H_{26}NO]^+$	267	41.3	$[M\text{-}15\text{-}15 + 2]^{2+}$	558	7.4	$[M]^+$	569	49.1	$[M + 2]^+$
231	4.5	$[L\text{-}15\text{-}15]^{2+}$	57	30.4	$[(CH_3)_3C]^+$	264	5.1	$[M\text{-}15\text{-}15]^{2+}$	260	23.8	$[C_{17}H_{26}NO]^+$
216	4.4	$[C_{14}H_{18}NO]^+$	260	18.1	$[C_{17}H_{26}NO]^+$	216	4.0	$[C_{14}H_{18}NO]^+$	250	3.4	
259	4.2		238	9.4		529	3.9	$[M\text{-}15\text{-}16]^+$	247	9.6	$[C_{16}H_{25}NO]^+$

Table 4 The TG data for salpren, Co(II), Ni(II), Cu(II), and Fe(II) complexes

Complex	C_p/ kJ g^{-1} °C^{-1}	T_p/°C	First step/°C	DTG_{max}/ °C	Mass loss, Δm calc./found/%	Second step/°C	DTG_{max}/ °C	Mass loss, Δm calc./found/%	Third step/°C	Residue	Calc./ found/%
Salpren	1.89	147.78	253–328	317	96.0 (–)	–	–	–	–	–	3.91 (–)
Ni(II) (salpren)	2.91	145.79	363–420	413	88.3 (86.9)	420–570	–	–	–	NiO	11.7 (13.1)
Cu(II) (salpren)	3.81	141.42	351–405	336	86.2 (87.2)	405–600	–	–	–	CuO	13.8 (12.8)
Co(II) (salpren)	2.35	147.53	329–420	380	85.2 (86.8)	420–610	–	–	–	CoO	14.8 (13.2)
Fe(II) (salpren)	2.50	151.57	162–190	181	3.6 (3.1)	346–375	361	81.1 (84.6)	375–610	FeO	15.3 (12.4)

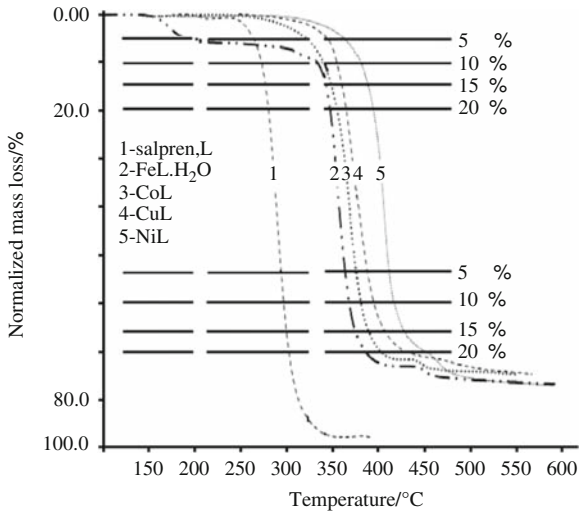

Fig. 3 The TG curves of ligand and its complexes

the complexes were calculated from DSC results and given in Table 4. The TG curves of the complexes are shown in Fig. 3 and were studied in greater detail. All complexes were studied by thermogravimetric analysis from ambient temperature to 700 °C in nitrogen atmosphere. The temperature ranges and percentage mass losses are given in Table 4, together with the temperatures of greatest rate of decomposition (DTG_{max}) and the theoretical percentage mass loss. Thermal curves obtained for most of the compounds were very similar in character. All complexes show two distinct steps mass loss except Fe(II) complex and salpren ligand [**L**] in their TG/DTG curves. Salpren ligand is one step and starts to decompose 253 °C and this step continues up to 328 °C. The TG curve of Co(II) complex indicates that the mass change begins at 329 °C and continuous up to 420 °C. The next decomposition step occurs in the temperature range 420–610 °C and corresponds to the formation of CoO (calc./found: 14.8/13.2%) (Table 4). The Ni(II) complex was stable up to 363 °C. The first step of thermal decomposition was completed at 420 °C. The second decomposition step starts to 420 °C and continues 570 °C. The solid residue was NiO (calc./found: 11.7/13.1%) (Table 3). The TG of Cu(II) complex reveal a mass loss in the temperature range 351–405 °C. The next decomposition step occurs in the temperature 405–600 °C and corresponds to the formation CuO (calc./found: 13.8/12.8%) (Table 4). Fe(II) complex is thermally stable up to 162 °C and undergoes decomposition beyond this temperature, as indicated by the first mass loss step in the TG curve. The mass loss at this temperature corresponds to elimination of H_2O (calc./found: 3.6/3.1%). The second decomposition step starts to 346 °C and continues 375 °C. After decomposition, the mass loss at 375–610 °C correspond to the formation of FeO (calc./found: 15.3/12.4%).

The end products were conformed with the XRD data. An as example the X-Ray pattern of the end product of Ni(II) complexes can be shown in Fig. 4.

The kinetic of heterogeneous condensed phase reactions that occur in nonisothermal conditions is usually described by equation,

$$\beta(d\alpha/dT) = Af(\alpha)\ \exp(-E/RT) \quad (1)$$

where α is the degree of conversion, β is the linear heating rate, and A is pre-exponential factor, and $f(\alpha)$ is the differential conversion function. For calculate kinetic parameters, the different reaction models may be used. The fraction mass loss, α and corresponding $(1-\alpha)^n$ are calculated from TG curves, where n depends upon the reaction

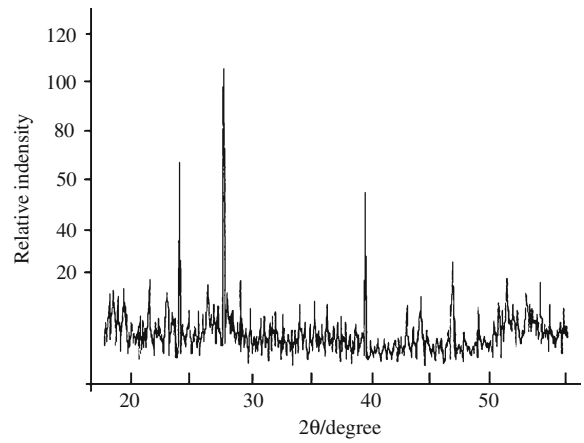

Fig. 4 X-Ray powder diffraction pattern of NiO

model. In studying the decomposition kinetic, five methods in the literature were chosen: Coats–Redfern (CR), Horowitz–Metzger (HM), van Krevelen (vK), MacCallum–Tanner (MC) and Madhusudanan–Krishnan–Ninan methods(MKN) and the methods may be expressed by following equations,

1. The Coats–Redfern method

$$\ln\left[g(\alpha)/T^2\right] = \ln[(AR/\beta E)(1-(2RT/E))] - (E/RT) \quad (2)$$

2. The van Krevelen method

$$\ln g(\alpha) = \left[A(0.368/T_m)^{E_a/RT_m}/\beta(E_a/RT_m+1)\right] + ((E_a/\mathrm{RT_m})+1)\ln T \quad (3)$$

3. The MacCallum–Tanner method

$$\log g(\alpha) = \log(AE/RT) - 0.4828\,E^{0.4351} - ((0.449 + 0.217\,E)/10^{-3}T) \quad (4)$$

4. The Madhusudanan–Krishnan–Ninan method

$$\ln[g(\alpha)/T^{1.9206}] = \ln(AE/RT) + (3.7678 - 1.9206\ln E - 0.12040(E/T)) \quad (5)$$

5. Horowitz–Metzger method

The Horowitz–Metzger method introduced a characteristic temperature T_m and a parameter Θ such that $\Theta = T - T_m$.

If the reaction order is 1, T_m is defined as the temperature at which $(1-\alpha)_m = 1/e = 0.368$ and the final expression is:

$$\ln\ln g(\alpha) = E\theta/RT_m^2$$

If the reaction order is unknown, T_m is defined for the maximum heating rate.

When $\Theta = 0$, $(1-\alpha) = (1-\alpha)_m$ and $(1-\alpha)_m = n^{1/1-n}$ and,

$$\ln g(\alpha) = \ln(ART_m^2/\beta E) - (E/RT_m) + (E\theta/RT_m^2) \quad (6)$$

A plot of $\ln g(\alpha)$ versus Θ can yield activation energy.

In the equations above, $g(\alpha)$, T_m, E, R, are the integral function of conversion, DTG peak temperature, activation energy (kJ mol^{-1}), and gas constant (8.314 J mol^{-1}K^{-1}), respectively. The kinetic parameters were calculated from the linear plots of the left-hand side of kinetic equations (Eqs 2, 4–6) against $1/T$, for van Krevelen equation (Eq. 3) the left-hand side is plotted against $\ln T$. The values E and A were calculated from the slope and intercept of the straight lines, respectively.

According to Coats and Redfern method, the plot of $\ln(g(\alpha)/T^2)$ versus $1/T$ gives straight line with slope equals to $-E/R$. The activation energies of complexes were calculated from the slope of Arrhenius curves and given Table 5. The second method of calculation of activation energy E, was developed by Madhusudanan–Krishnan–Ninan. According to this method, a relationship between $\ln(g(\alpha)/T^{1,9206})$ versus $1/T$ in same conditions is constructed. The other method used to calculate the activation energies is that of MacCallum–Tanner. The activation energy of decomposition can be thus determined by Eq. 4. From the plot it is possible calculate the activation energies from the slopes. The activation energies of the ligand and complexes are between 114.3 and 276.1 kJ mol^{-1}. The activation energy was also determined by the method of van Krevelen in nitrogen for mass loss thermograms of 10 °C min^{-1} and can calculated from slopes of the log $g(\alpha)$ against $\ln T$ plot. Finally, in case of Horowitz–Metzger method the activation energies were calculated from the slopes of the $\ln g(\alpha)$ versus Θ plots as 245.36, 156.43, 145.33, 176.94 and 168.32 kJ mol^{-1}.

For all methods, determination of the pre-exponential factor and reaction order is possible from the expression of $g(\alpha)$ in Eq. 3 and $n \neq 1$:

$$g(\alpha) = 1 - (1-\alpha)^{1-n}/1-n$$

Moreover, Table 5 summarizes the reaction orders, pre-exponential factors, correlation coefficients and the activation energies obtained by the five different methods examined in this study. The results are in good agreement with the values obtained from all of them. The results indicate that the values of all methods are comparable. They are similar to the values given in the literature for salpren ligand and metal complexes.

As seen in Table 5, the value of correlation coefficients of linearization curves of salpren ligand and metal complexes are approximately 1.00 and values of reaction orders are around 1.00 for complexes. The kinetic data obtained by different methods agree with each other.

The enthalpy $\Delta H^{\#}$, activation entropy $\Delta S^{\#}$, and the free energy of activation $\Delta G^{\#}$, of the complexes and salpren ligand were calculated using the following relations [21]:

$$\Delta S^{\#} = 2.303\log(Ah/kT)R, \Delta H = E - RT, \Delta G^{\#} = \Delta H - T\Delta S^{\#}$$

where h is the Planck constant and T is the temperature, A is the pre-exponential factor. The thermodynamic parameters calculated were reported in Table 5.

Table 5 The kinetic data on metal complexes of salpren

Method	Complexes	n	E/kJ mol^{-1}	ln A/min^{-1}	Correlation coefficient, r	$\Delta S^{\#}$/J mol^{-1} K^{-1}	$\Delta H^{\#}$/J mol^{-1} K^{-1}	$\Delta G^{\#}$/J mol^{-1} K^{-1}
CR	Salpren ligand	0.7	111.8	22.79	0.99934	−61.12	106.89	142.95
	Ni(II) salpren	1.1	170.3	28.79	0.99818	−12.45	164.60	173.13
	Cu(II) salpren	0.7	207.6	47.00	0.99748	139.2	202.04	108.90
	Co(II) salpren	0.8	147.9	24.65	0.99643	−46.45	142.47	172.81
	Dehydradation	0.9	197.3	50.35	0.99621	170.2	193.53	116.22
	Fe(II) salpren	0.7	219.6	39.67	0.99790	78.68	214.33	164.44
MKN	Salpren ligand	0.7	112.1	20.63	0.99935	−79.09	107.19	153.86
	Ni(II) salpren	1	176.8	27.63	0.99838	−22.12	171.11	186.27
	Cu(II) salpren	0.7	272.1	46.97	0.99750	138.8	266.54	173.62
	Co(II) salpren	1	164.9	26.16	0.99787	−33.96	159.47	181.63
	Dehydradation	1	211.1	52.23	0.99636	185.8	207.33	122.96
	Fe(II) salpren	0.7	219.8	39.73	0.99791	79.16	214.53	164.34
MC	Salpren ligand	0.7	114.3	29.14	0.99944	−8.357	109.39	114.33
	Ni(II) salpren	1.1	173.4	78.38	0.99476	399.9	167.71	−106.61
	Cu(II) salpren	0.7	276.1	56.33	0.99768	216.7	270.54	125.56
	Co(II) salpren	0.7	147.7	32.98	0.99821	22.75	142.27	127.41
	Dehydradation	0.9	196.4	58.70	0.99649	239.6	192.63	83.831
	Fe(II) salpren	0.7	222.7	48.76	0.99809	154.2	217.43	119.64
HM	Salpren ligand	1	149.4	12.15	0.99925	−149.6	144.49	232.73
	Ni(II) salpren	1.4	219.7	12.71	0.99848	−146.2	214.00	314.31
	Cu(II) salpren	0.8	302.3	12.74	0.99734	−145.8	296.74	394.25
	Co(II) salpren	1.2	183.9	11.78	0.99665	−153.6	178.47	278.74
	Dehydradation	1	215.7	12.15	0.99612	−147.4	211.93	278.83
	Fe(II) salpren	0.9	254.1	12.51	0.99812	−147.2	248.83	342.17

The activation energy and Gibbs free energy of the complexes is expected to increase proportional to the decrease in their radii. Complexes of Cu, Ni and Co have a square-planar geometry and show similar decomposition steps, the smaller size of Cu(II) as compared to Co(II) and Ni(II) permits a closer approach of the ligand to Cu(II) ion. Hence the E value for the Cu(II) complex is higher than that of Co(II) and Ni(II). The E values for thermal decomposition with respect to the above methods can be put into a descending order as, $E_{Cu} > E_{Ni} > E_{Co}$. The activation energies corresponding decomposition steps are in the range of 111.8–302.3 kJ mol^{-1} which indicates in this order: Ni(II) > Cu(II) > Co(II). The negative values of $\Delta S^{\#}$ in the studied complexes indicate that the reaction rates are slower than normal.

Conclusions

DIP-MS was found to be very powerful technique to characterize complex structure. It was noticed that doubly charged ion stability occurred by two methyl groups leaving from both sides of the ligand and its metal ion complexes was really high. This is the case of the location of these two doubly positive charged ion enough far away from each other due to the bulky structure of the species. Isotopic distribution of the metal complexes of the ligand was yielded new information to evaluate of the exact fragmentation of the complex especially for the doubly charged ion stability. The TGA curves of all the compounds show almost a similar decomposition when heated about 700 °C. The complexes prepared with different metals decompose in two-step process. Using the CR, HM, MT and MKN methods performed kinetic analysis of the thermogravimetric data. The activation energies obtained by non-isothermal conditions are compared. The thermal stabilities of metal complexes of salpren ligand were found as Ni(II) > Cu(II) > Co(II) > Fe(II). These study show that there is a relationship between the ionic radius of the metal and the thermal stability of the complex [22, 23]. The melting points of the complexes increase in order; Fe(II) > salpren > Co(II) > Ni(II) > Cu(II) corresponding the numerical values in Kelvin; 151.57, 147.78, 147.53, 145.79 and 141.42 in same order.

Acknowledgements The authors gratefully acknowledge Basri Gülbakan and Ömür Çelikbıçak for helpful Mass Spectrometry measurements.

References

1. Sheldon RA, Kochi JR. Metal catalyzed oxidation of organic compounds. New York: Academic Press; 1981.
2. Kaim W. The transition metal coordination chemistry of anion radicals. Coord Chem Rev. 1987;76:187–235.
3. Halfen JA, Toung VG, Tolman WB. Modeling of the chemistry of the active site of galactose oxidase. Angew Chem Int Ed. 1996;35(15):1687–90.
4. Zhang W, Loebach JL, Wilson SR, Jacobsen EN. Enantioselective epoxidation of unfunctionalized olefins catalyzed by salen manganese complexes. J Am Chem Soc. 1990;112(7):2801–3.
5. Kumar DN, Garg BS. Some new cobalt(II) complexes: synthesis, characterization and thermal studies. J Therm Anal Calorim. 2002;69:607–16.
6. Wang HD, Li YT, Ma PH, Zeng XC. Studies on the thermal decomposition of *N*,*N*′-ethylenebis(salicylideneiminato) diaquochromium(III) nitrate. J Therm Anal Calorim. 2002;69(2):575–81.
7. Doğan F, Gülcemal S, Yürekli M, Çetinkaya B. Thermal analysis study of imidazolinium and some benzimid azolium salts by TG. J Therm Anal Calorim. 2008;91(2):395–400.
8. Doğan F, Dayan O, Yürekli M, Çetinkaya B. Thermal study of ruthenium(II) complexes containing pyridine-2,6-diimines. J Therm Anal Calorim. 2008;91(3):943–9.
9. Kasumov VT, Yaman OS, Tas E. Synthesis, spectroscopy and electrochemical behaviors of nickel(II) complexes with tetradentate shiff bases derived from 3,5-But2-salicylaldehyde. Spectrochim Acta A. 2005;62(1–3):716–20.
10. Coats AW, Redfern JP. Kinetic parameters from thermogravimetric data. Nature. 1964;201:68–9.
11. van Krevelen DW, van Heerden C, Huntjons FJ. Kinetic study by thermogravimetry. Fuel. 1951;30:253–8.
12. MacCallum JR, Tanner J. Derivation of rate equations used in thermogravimetry. Nature. 1970;225(5238):1127–8.
13. Madhusudanan PM, Krishnan K, Ninan KN. New equations for kinetic analysis of non-isothermal reactions. Thermochim Acta. 1993;221:13–21.
14. Horowitz HH, Metzger G. New analysis of thermogravimetric traces. Anal Chem. 1963;35:1464–8.
15. Larrow JF, Jacobsen EN, Gao Y, Hong Y, Nie X, Zepp CM. A practical method for the large-scale preparation of [*N*,*N*′-Bis(3,5-di-tertbutylsalicylidene)-1,2-cyclohexanediaminato (2-)]manganese(III) chloride, a highly enantioselective epoxidation catalyst. J Org Chem. 1994;59(7):1939–42.
16. Earnshaw A. Introduction to magnetochemistry. London: Academic Press; 1968.
17. Tas E, Aslanoglu M, Guler M, Ulusoy M. Synthesis, spectral characterization and electrochemical studies of copper(II) and cobalt(II) complexes with novel tetradentate salicylaldimines. J Coord Chem. 2004;57(8):583–9.
18. Temel H, Sekerci M. Novel complexes of manganese(III), cobalt(II), copper(II), and zinc(II) with Schiff base derived from 1,2-bis(*p*-aminophenoxy)ethane and salicylaldehyde. Synth React Inorg Met-Org Chem. 2001;31(5):849–57.
19. Sacconi L, Ciampolini M, Maggio F, Cavasino FP. Studies in coordination chemistry. IX.[1] Investigation of the stereochemistry of some complex compounds of cobalt(II) with N-substituted salicylaldimines. J Am Chem Soc. 1962;84(17):3246–8.
20. Mukherjee RN, Abrahamson AJ, Patterson GS, Stack TDP, Holm RH. A new class of (*N*,*N*′-bis(salicylideneamino)ethanato)iron(II) complexes-5-coordinate [FeII(salen)L]- preparation, properties, and mechanism of electron-transfer reactions. Inorg Chem. 1988;27(12):2137–44.
21. Straszko J, Humienik MO, Mozejko J. Study of the mechanism and kinetic parameters of the thermal decomposition of cobalt sulphate hexahydrate. J Therm Anal Calorim. 2000;59(3):935–42.
22. Sodhi GS. Correlation of thermal-stability with structures for some metal-complexes. Thermochim Acta. 1987;120:107–14.
23. Nagase K, Sato K, Tanaka N. Thermal dehydration and decomposition reactions of bivalent metal oxalates in the solid state. Bull Chem Soc Jpn. 1975;48(2):439–42.